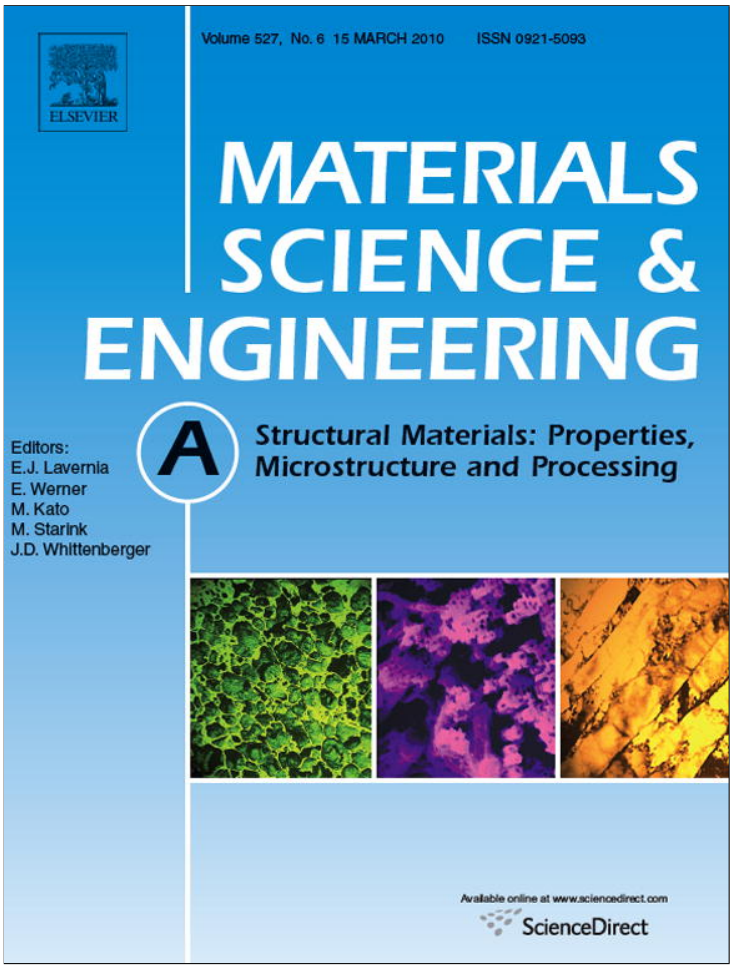

Materials Science and Engineering A 527 (2010) 1299–1305

Contents lists available at ScienceDirect

Materials Science and Engineering A

journal homepage: www.elsevier.com/locate/msea

Influence of hot deformation strain rate on the mechanical properties and microstructure of K310 cold work tool steel

H.R. Ezatpour, S.A. Sajjadi*, M. Haddad-Sabzevar

Department of Metallurgy and Materials Engineering, Faculty of Engineering, Ferdowsi University of Mashhad, Mashhad 91775-1111, Iran

ARTICLE INFO

Article history:
Received 28 May 2009
Received in revised form
24 September 2009
Accepted 11 November 2009

Keywords:
Tool steel
K310
Hot deformation
Dynamic recovery
Dynamic recrystallization

ABSTRACT

K310 is a cold work tool steel used in manufacturing of forging dies. To study hot deformation behavior and flow stress model of the steel, continuous hot compression tests in the range of 900-1100 °C with strain rates of 0.01, 0.1 and 1 s^{-1} were performed. The dependency of the peak stress, initial stress, steady state stress, peak strain and dynamic recrystallization on Zener-Holloman parameter was determined. It was shown that the function relating stress and strain rate is generally the hyperbolic sine, since the power and exponential laws lose linearity at high and low stresses, respectively. The microstructural results showed that decreasing strain rate and increasing temperature (low *Z*) lead to decrease in peak strain and peak stress and activation energy for dynamic recrystallization. Meanwhile graph analyzes showed that the necklace structure is developed and grains become finer. Also, hardness results indicated that with increasing strain rate and decreasing temperature (high *Z*), the hardness is increased. At high temperature and strain rate, existence of cavities in grain boundaries indicated decreasing grain boundary sliding.

1. Introduction

Generally, plain carbon steels can be worked without great difficulty, since they can be preheated to single phase austenite easily and worked through the required stages of reduction before any transformation or precipitation taking place. The dissolved C in austenite usually increases the hot workability, since it promotes the self diffusion of Fe in the lattice, thus enhancing dynamic recovery without interfering with dynamic recrystallization [1–3].

On the other hand, in most alloy steels solute strengthening occurs because preheating normally takes the alloying elements into solution. The effects of solute increase with increasing the total metallic alloying concentration [4–6]. In certain tool steels the level and nature of metallic elements and carbon content are such that carbides are not dissolved in the common working range, making them more difficult to deform. Good examples are the cold work (A) and high-speed (M) tool steels [7–9].

Cold work steels are usually austenitized for heat treating in the range 920- 980 °C, in which the carbides are dissolved and hence no change occurs when the working temperature is above this range. In the M grade steels even when austenitized at 1190–1290 °C, the particles of M_6C [$Fe_3(W,Mo)_3C$–$Fe_4(W,Mo)_2C$] are not completely dissolved, and their quantity limits the workability as compared to plain carbon steels.

After yielding, strain hardening takes place. The effects of strain hardening are counterbalanced by dynamic recovery (DRV) and subsequently (in some materials), by the simultaneous occurrence of dynamic recrystallization (DRX) [10–12]. As deformation begins, dislocations form tangles which through DRV at about 10% strain polygonize into subgrain boundaries [13,14]. Materials with high stacking fault energy (SFE) recover readily, so that equilibrium is reached between work hardening and softening due to the recovery. The stress–strain curves of these metals, in hot working, show stress increasing progressively and finally levels off in a steady state to a plateau. Transmission electron microscopy (TEM) studies have clearly identified that there is an equiaxed substructure with low misorientations within the original elongated grains [10,15]. Metals with low SFE, such as the austenitic state steels, do not undergo DRV readily, so that the accumulation of dislocations with high local concentrations leads to DRX which commences at strains just before the peak.

Although hot working properties of cold work tool steels such as K310 is of great interest from both fundamental and industrial view points, there are comparatively few researches reported in the scientific literature [16,17]. The objective of this research is to investigate the hot working characteristics of cold work tool steel type K310 by continuous compression tests at different strain rates and temperatures to determine the effect of dynamic recovery and recrystallization on flow stress, hot workability and ductility.

* Corresponding author at: Department of Metallurgy and Materials Engineering, Faculty of Engineering, Ferdowsi University of Mashhad, Mashhad, Iran.
Tel.: +98 511 8763305; fax: +98 511 8763305.
E-mail address: sajjadi@um.ac.ir (S.A. Sajjadi).

0921-5093/$ – see front matter © 2009 Elsevier B.V. All rights reserved.
doi:10.1016/j.msea.2009.11.027

2. Experimental techniques

The chemical composition of the cold work tool steel K310 supplied for this project was determined using Optical Emission Spectroscopy (OES) technique. The compression test specimens 15 mm in length and 10 mm in diameter ($H/D = 1.5$) were machined from hot work bars.

Continuous compression tests were performed at strain rates of 0.01, 0.1 and 1 s^{-1} and at temperatures of 900, 950, 1000, 1050 and 1100 °C to a true strain of 0.8. The specimens were heated rapidly by means of a cylindrical element furnace to the test temperature and held for 15 min before deforming. At the end of test, specimens were withdrawn from the furnace rapidly and quenched in water.

The hardness was measured by Vickers method to investigate dynamic recrystallization.

The longitudinal and transverse sections of the specimens were used for metallographic analysis. The surfaces were prepared by mechanical polishing and etching in Vilella agent (5 ml HCL, 1 g picric acid and 100 ml ethyl alcohol) and examined using an Optical Microscope. Carbide volume fraction was determined by point counting according to ASTM E562-89. Grain sizes were determined by the three-circle intercept method according to ASTM E112.

3. Results and Discussion

The chemical composition of K310 steel, in weight percent, is given in Table 1. The representative stress–strain curves for K310

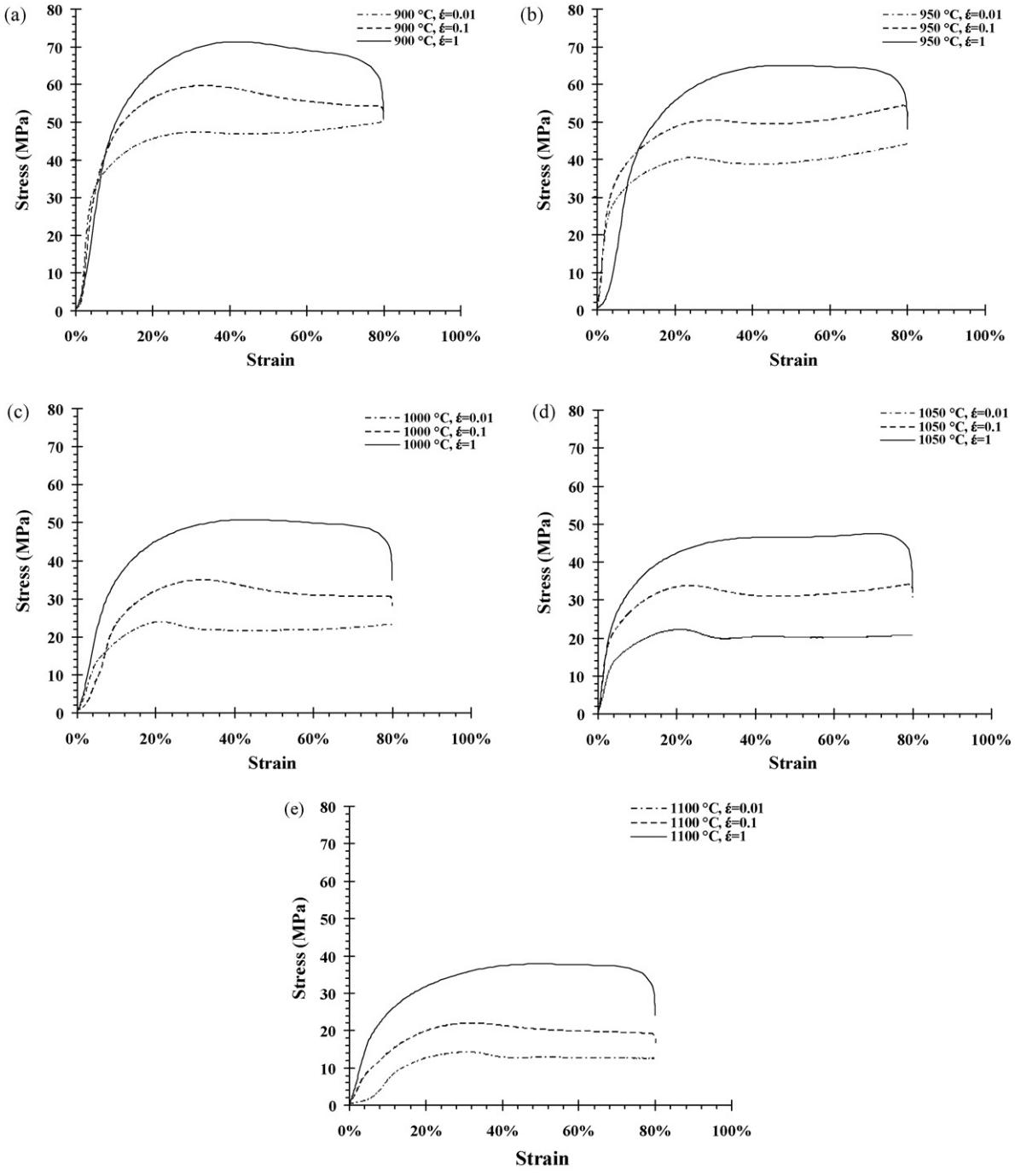

Fig. 1. Representative stress–strain curves of K310 tool steel tested in compression at different temperatures; (a) 900 °C, (b) 950 °C, (c) 1000 °C, (d) 1050 °C and (e) 1100 °C at strain rate of 0.01, 0.1 and 1 s^{-1}.

Table 1
Chemical composition (wt.%) and original grain size (μm) of K310 tool steel.

AISI	C	Mn	Mo	Cr	Si	Grain size
K310	0.83	0.4	0.3	1.9	0.45	140

steel in the temperature range of 900-1100 °C and strain rate of 0.01, 0.1 and 1 s^{-1} are presented in Fig. 1. The equivalent stress, σ, and strain, ε, were calculated according to the following formulas:

$$\sigma = \frac{F}{A}(\mathrm{N/mm^2}) \quad \text{and} \quad \varepsilon = \ln\left(\frac{h}{h_0}\right) \tag{1}$$

when h_0 is the initial height and h is the final height.

Cold work steels, throughout the experimental regime, exhibit the classical behavior of materials, which undergo dynamic recrystallization (DRX) strain hardening to the peak stress, σ_p, and then work softening towards a steady state stress, σ_{ss}. The end of work softening is considered to be the completion of the first wave of recrystallization, which proceeds by nucleation of new grains until initial grains are consumed. The behavior changes markedly in the steady state, i.e., distributed DRX in conjunction with dynamic recovery (DRV) which results in grains of constant size and average dislocation density.

The critical stress for initiation of DRX, σ_c, is obtained from θ–σ curves, where θ is the strain hardening rate, $d\sigma/d\varepsilon$. The ratio of critical strain to peak strain ($\varepsilon_c/\varepsilon_p$) is varying between 0.6 and 0.7, with the larger ratios at higher temperatures. Both critical and peak strains decrease with decreasing peak stress [2,17].

In the austenitic state the hot workability of plain carbon steels improves with increasing carbon concentration [3,18]. Temperature, strain rate and strain are very important in forging and forming processing [1,16]. The flow curves (Fig. 1) for K310 steel exhibit a peak and then softening to the steady state, i.e., characteristic of DRX in conditions of low strain rate and high temperature (low Z). In the contrary, at high strain rate ($\dot{\varepsilon} = 1$), the flow curves for K310 steel exhibit work hardening up to the steady state, i.e., characteristic of DRV. The peak stresses of tool steels, as well as homogenized wrought austenitic stainless steels, are in general much higher than carbon and HSLA steels. The alloys contain considerably greater amounts of alloying elements. Solute atoms exert a drag on dislocations, reducing their mobility, thus decrease DRV and increase strain hardening. They also exert a drag on gain boundaries which impede grain boundary migration and show softening by DRX, and consequently, increasing the strength [15,18]. The critical strain for starting DRX in tool steels is close to that of as-cast stainless steel.

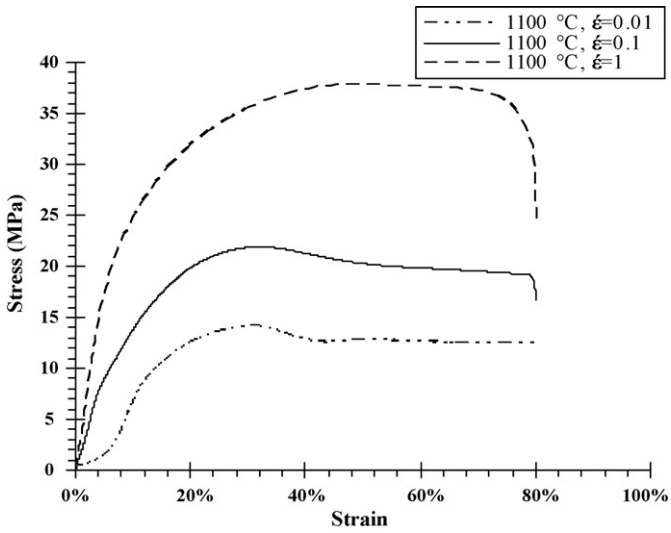

Fig. 2. Representative stress–strain curves of K310 tool steels tested in compression at temperature 1100 °C and strain rate of 0.01, 0.1 and 1 s^{-1}.

The effect of decreasing strain rate at a constant stress at 1100 °C on the σ–ε curve is typically to lower the flow stress as shown in Fig. 2. The figure also indicates that the restoration mechanism changes from dynamic recrystallization (DRX) at low stress and low strain rates to dynamic recovery at high stresses and high strain rates. Dynamic recovery and recrystallization are important, because the interaction of the softening process and fracture mechanism determines the ductility during hot working. DRX is extremely important in raising the hot workability by separating cracks from the grain boundaries, by grain boundary migration, so that crack growth is impeded and crack blunting occurs [4,13]. At constant temperature, by increasing strain rate the effect of dislocation production is overcome, making dynamic recovery the softening mechanism (Fig. 2). If all deformation conditions, except

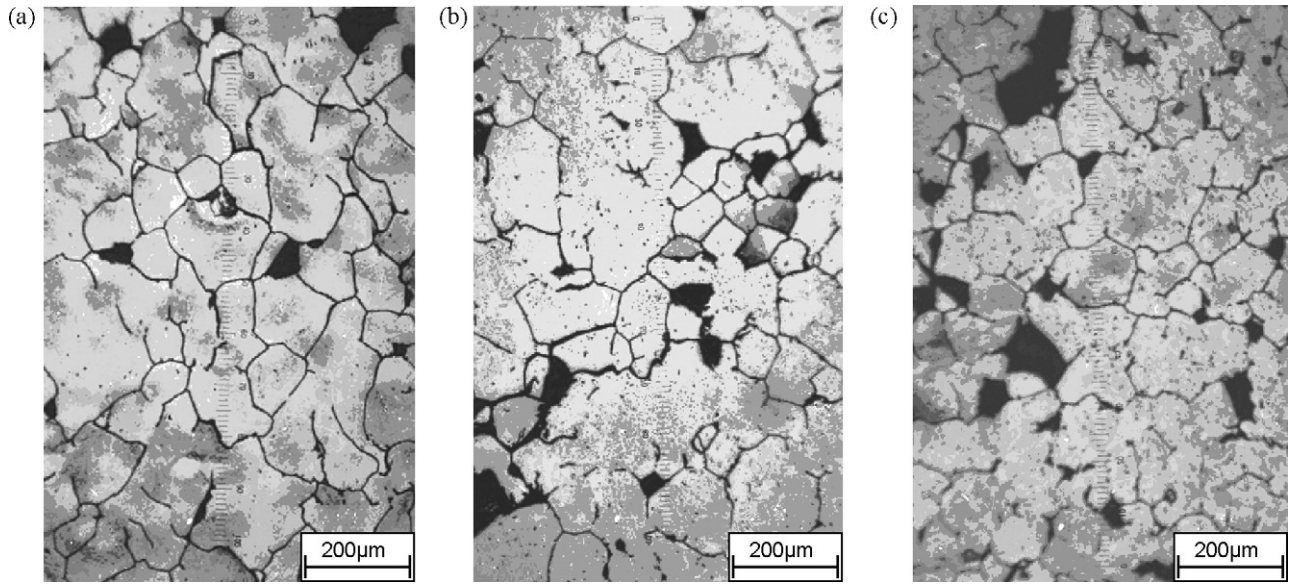

Fig. 3. Optical micrographs of the DRX grains of K310 steel deformed at 1100 °C and quenched in water at strain rate of (a) 0.01 s^{-1}, (b) 0.1 s^{-1} and (c) 1 s^{-1}.

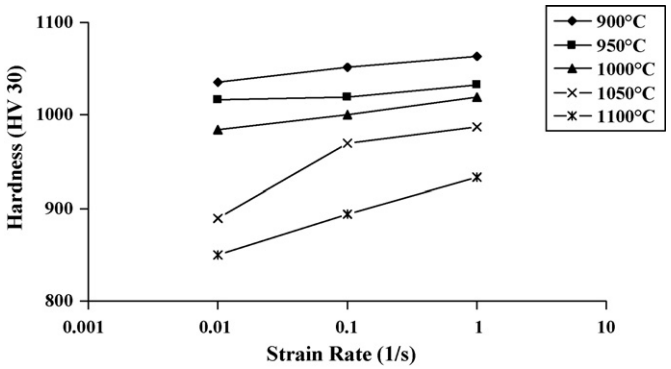

Fig. 4. Representative hardness results of K310 tool steels tested in compression in the range of 900–1100 °C at strain rate of 0.01, 0.1 and 1 s^{-1}.

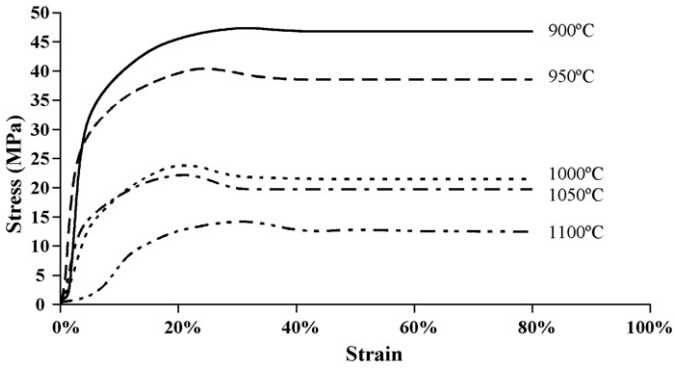

Fig. 5. Representative stress–strain curves of the K310 tool steels tested in compression at temperatures of 900, 950, 1000, 1050 and 1100 °C at strain rate of 0.01 s^{-1}.

strain rate, are fixed, then:

$$\ln\left(\frac{\dot{\varepsilon}_2}{\dot{\varepsilon}_1}\right) = \frac{\sigma_2}{\sigma_1} \quad (2)$$

Therefore, the flow stress, peak stress and steady state stress increase with increasing strain rate. After the peak, the σ–ε curve declines at a relatively constant slope and then experiences a perceptible inflection, where the first wave of DRX is effectively complete and the steady state regime commences. With decreasing strain rate, grains are finer and more uniform. The fact is confirmed by metallographic results (Fig. 3a–c).

The hardness results indicate that hardness decreases with decreasing strain rate (Fig. 4). The results show that work softening and DRX content increase with decreasing strain rate, which correspond to the metallographic and curves analysis.

Stress–strain curves at 900, 950, 1000, 1050 and 1100 °C and strain rate of 0.01 s^{-1} are presented in Fig. 5. With increasing temperature, peak stress and strain and steady state stress decrease. The work softening and dynamically recrystallized portions increase in K310 steel.

Metallographic examinations show that, with increasing temperature from 1050 to 1100 °C, grains become finer and uniform (Figs. 6 and 7). Also, at high temperatures, carbides are not observed at grain boundaries and inside of grains. The hardness results (Fig. 4) indicate that, hardness decreases with increasing temperature.

The increase in strength of alloy steels is more influenced by the presence of carbides as compared to solution of the alloying elements in the austenite matrix [15,16]. The strengthening effect of alloying elements in the form of carbides can be illustrated by the fact that at 1100 °C, K310 steel just benefits from 0.62% volume fraction carbide while at 900 °C there is 4.2% volume fraction of carbides. The strengthening effects of the second phase particles depend on their size, distribution and strength relative to the matrix. Fine particles (<0.5 μm) retard nucleus growth by reducing grain boundary migration [15,18]. With increasing temperature, the carbides are dissolved and recrystallization reduces in K310 steel, while grains are finer and more uniform than at lower temperature and higher strain rate (Figs. 3, 6 and 7). The rate of DRX for K310 steel is lower than A_2 and M_2 steels because of the lower carbides in this steel.

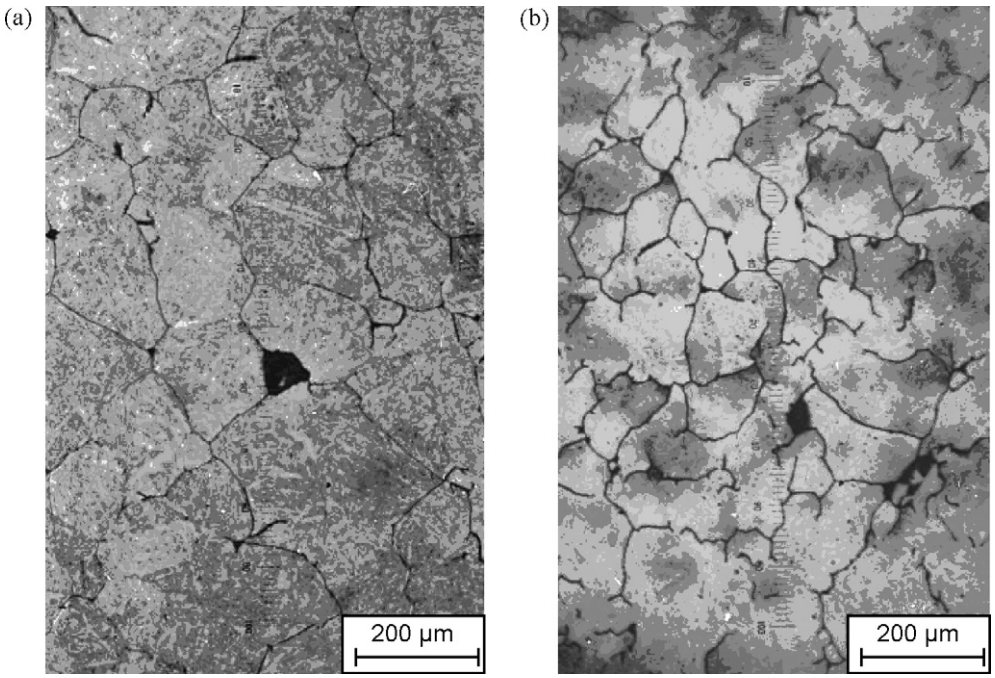

Fig. 6. Optical microstructures of the specimens held at 1050 °C for 15 min and quenched in water: (a) before deformation and (b) after deformation at 0.01 s^{-1}, showing DRX grains.

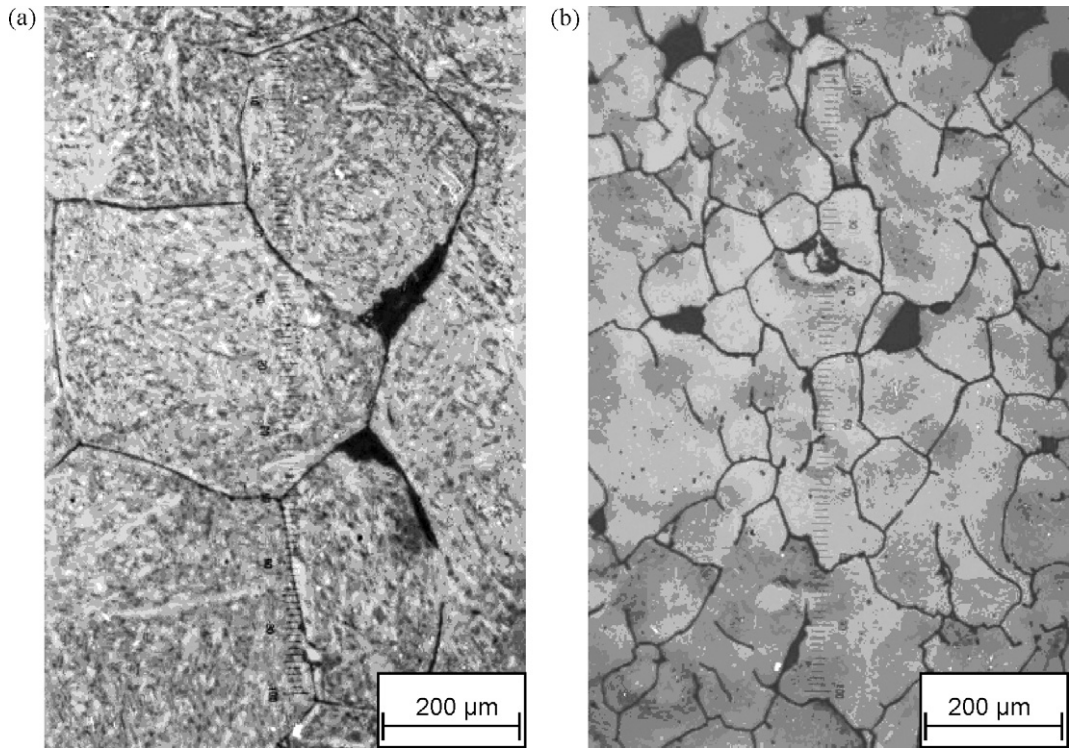

Fig. 7. Optical microstructures of the specimens held at 1100 °C for 15 min and quenched in water: (a) before deformation and (b) after deformation at 0.01 s^{-1}, showing DRX grains.

Two types of carbides, $M_{23}C_6$ and M_6C, are found in the K310 steel [4,18]. Depending on the metallic alloying elements in tool steels, these carbides have certain amount of solubility. Carbide compositions depend on the relative amounts of alloying elements and heat treatment cycle. The chromium-rich $M_{23}C_6$ carbide dissolves readily and possesses microhardness of the order of 1200 HV 0.02. The M_6C carbide is tungsten or molybdenum-rich carbide considerably harder than $M_{23}C_6$, with about 1500 HV 0.02, and does not readily dissolve in the matrix at working temperature. The total carbide content of steel and its decline with rising temperature have a strong influence on hot strength and ductility of the steel [4,7]. Table 2 gives the volume fraction of the carbides at different temperatures in the K310 steel determined by point counting method.

The effect of temperature on peak stress is shown in Fig. 8. The peak stress decreases as temperature increases. The influence of temperature and strain rate on peak stress was analyzed by the following equations, which were originally developed for creep, but have found applicability at high strain rates in hot working [1,8,19]:

$$A'\sigma_p^{n'} = \dot{\varepsilon}\exp\left(\frac{Q_{HW}}{RT}\right) = Z \quad (3)$$

$$A''\exp\left(\beta\sigma_p\right) = \dot{\varepsilon}\exp\left(\frac{Q_{HW}}{RT}\right) = Z \quad (4)$$

$$A\left[\sinh\left(\alpha\sigma_p\right)\right]^n = \dot{\varepsilon}\exp\left(\frac{Q_{HW}}{RT}\right) = Z \quad (5)$$

where $A, A', A'', n, n', \alpha, \beta, Q_{HW}$ and R are constants and Z is the Zener-Holloman parameter. Q_{HW} is the activation energy of hot working and R is the universal gas constant. A power law gives linear segment only at low stresses, indicating the limited applicability of Eq. (3). However, in the law of $\beta\sigma_p$ against $\log Z$ (Eq. (4)) linearity is lost at low stresses. Eq. (5) is a more general form of Eq. (3) for low stresses, and Eq. (4) for high stresses, as shown in Fig. 9. When the peak stress is plotted according to the hyperbolic sine equation good agreement is found for K310 steel as shown in Fig. 10a with the parallel temperature lines for each alloy. The slope n is 3.8 for K310 steel and 3.6 and 3.4 for A_2 and M_2 steels, respectively. The distance between the parallel lines increases with decreasing temperature. A semi-logarithmic plot of the peak stress term versus the reciprocal of the absolute temperature, i.e., $\log(\sinh(\alpha\sigma_p))$ versus $(1/T)$, also found good agreement with parallel lines for the alloy. The slopes of these sets of lines for K310 steel are presented in Fig. 10b.

Existence of voids at high strain rate indicates that grain boundary sliding has decreased [11,14]. Therefore, tool steels have low

Table 2
Carbide volume fraction at different temperatures.

	900 °C	1000 °C	1100 °C
$M_{23}C_6$	3.4%	2.2%	0.3%
M_6C	0.8%	0.6%	0.32%

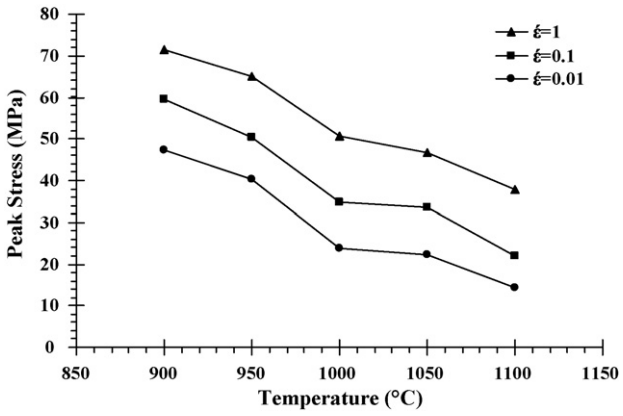

Fig. 8. Peak stress, σ_p, as a function of temperature for specimens tested in compression in the temperature range of 900–1100 °C at different strain rates.

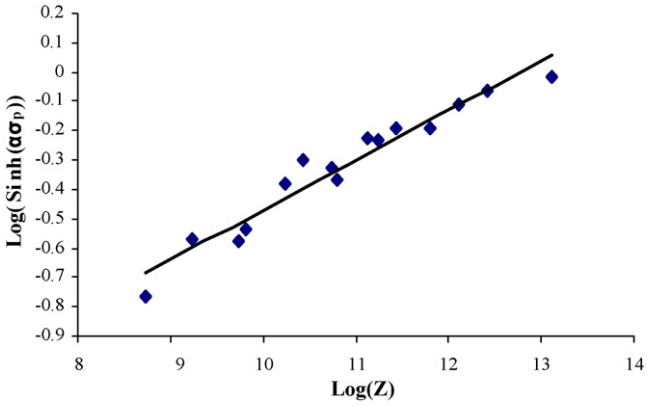

Fig. 9. Logarithmic plots of the peak stress sinh function versus temperature compensated strain rate Z according to Eq. (5), for tool steel K310.

fracture strains because of the readily formation of voids in carbides or carbide–matrix interfaces due to the fracture or decohesion of the particles [1,2,4]. The dependence of the peak stress on temperature and strain rate is demonstrated by the good fit of the hyperbolic sine function in Fig. 9, which is in good agreement with other works [2,9]. The value of the stress exponent, n, varies between 2 and 5 for steels and decreases as the alloy strength increases [2,9]. This is reflected in higher value of n for K310 tool steel, being 3.8 as compared to 3.6 and 3.4 for A_2 and M_2 steels, respectively. The value of n depends on the value of α used in hyperbolic sine function (Eq. (5)). So, comparisons must take this into consideration. Analysis of the tool steels data indicates that the value of $\alpha = 1.2 \times 10^{-2}\ \mathrm{MPa}^{-1}$ can be used for all steels with strength comparable to the K310 tool steel [5,7,18].

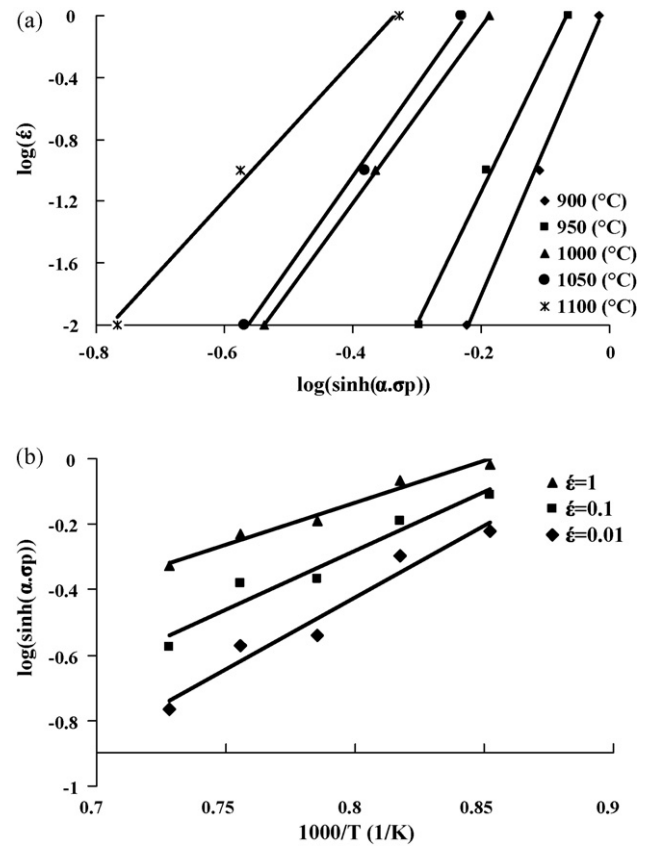

Fig. 10. (a) Logarithmic plots of the strain rate versus log sinh function of the peak stress. (b) Plots of log sinh function of the peak stress versus the reciprocal of the absolute temperature.

The hot working activation energy Q_{HW} can be calculated with these slopes and the stress exponent n determined previously for K310 tool steel. The activation energy determined is 226.88 kJ/mol for K310 steel, while these are 399 and 455 kJ/mol for A_2 and M_2 steels. The activation energy for K310 steel is lower than A_2 and M_2 steels due to the lower hard carbides in this steel. The stress exponent is a function of strength, and decreases with increasing strength. Therefore, stress exponent for K310 steel is higher than that for A_2 and M_2 steels.

There is also very good fit with Arrhenius function (Fig. 10) providing activation energy, Q_{HW}, for the entire temperature regime. Q_{HW} increases with alloy content as solute and/or precipitate makes the operation of the deformation and recovery mechanism more difficult, thus causing greater strength at decreased temperatures [1,2,20]. K310 steel has activation energy of about 226.88 kJ/mol, whereas the value for low alloy steels is around 300 kJ/mol. HSLA steels have values of 330–450 kJ/mol due primarily to the carbonitrides, which precipitate between 950 and 800 °C, whereas austenite stainless steels with their high solute content have much higher activation energies, from 350 to 510 kJ/mol [3,5,20]. In M_2 steels there are a lot of hard M_6C carbide precipitates in comparison to K310 steel which contains greater amount of the softer $M_{23}C_6$ precipitates. Consequently, the activation energy of M_2 is greater than that of K310 steel, which is 455 and 226.88 kJ/ml, respectively [7,16].

4. Conclusions

The following results were obtained from the investigation on the hot deformation properties of K310 cold work tool steel:

- Temperature, strain rate and strain are very important factors in forging and forming processes at high temperatures.
- The flow curves for K310 steel exhibit a peak and then softening to the steady state, i.e., characteristic of DRX in condition of low strain rate and high temperature (low Z), and at high strain rate ($\dot{\varepsilon} = 1$).
- The flow curves for K310 steel exhibit work hardening up to the steady state, i.e., characteristic of DRV.
- Metallographic studies and curves analysis showed DRX percent is increased by decreasing strain rate.
- With increasing temperature, peak stress, strain at the peak and steady state stress decrease. Also, the work softening and recrystallization percent in K310 steel increased.
- n-Value for K310 tool steel is 3.8, as compared to 3.6 and 3.4 for A_2 and M_2 steels, respectively.
- Hot working activation energy for K310 steel is 226.88 kJ/mol.

Acknowledgements

The authors wish to express appreciation to the Steel Complex of Esferaien for supporting this project. Also, Dr. Ebrahimi from University of Sabzevar, is gratefully acknowledged for helping in performing tests.

References

[1] H.J. McQueen, Metall. Mater. Trans. A 33A (2002) 345.
[2] H.J. McQueen, N.D. Ryan, Mater. Sci. Eng. A A322 (2002) 43.
[3] N. Cabanas, N. Akdut, J. Penning, B.C. DeComan, Metall. Mater. Trans. A 37A (2006) 3305.
[4] C.A.C. Imbert, H.J. McQueen, Can. Metall. Q. 40 (2) (2001) 235.
[5] E. Evangelista, H.J. McQueen, M. Niewczas, M. Cabibbo, Can. Metall. Q. 43 (3) (2004) 339.
[6] B. Voyzelle, PhD Thesis, Queen's University, Kingston, Ontario, Canada, 1999, pp. 1–205.

[7] C.A.C. Imbert, H.J. McQueen, Mater. Sci. Eng. A A313 (2001) 88.
[8] I. Perus, G. Kugler, M. Tercelj, P. Fajfar, Metalurgija 44 (2005) 261.
[9] C.A.C. Imbert, N.D. Ryan, H.J. McQueen, Metall. Trans. A 15A (1984) 1855.
[10] T. Tran, N.D. Ryan, H.J. McQueen, M.E. Smagorinsky, ibid, 240 (1996) 317.
[11] S.K. Samanta, Deformation under Hot Working Conditions Conf. Proc., Sheffield University, ISI Publication Vol. 108, The Iron and Steel Institute, 1968, p. 122.
[12] F.J. Humpheys, M. Hatherly, Recrystallization and Related Annealing Phenomena, 1966, Pergamon.
[13] N.D. Rayan, Proc. of Int. Conf., CIM, 1996, p. 411.
[14] L.E. Murr, E.V. Esqueivel, J. Mater. Sci. 39 (2004) 1153.
[15] M. Mataya, E. Nilsson, E. Brown, G. Krauss, Metall. Mater. Trans. A 34A (2003) 3021.
[16] C.A.C. Imbert, H.J. McQueen, Mater. Sci. Eng. A A313 (2001) 104.
[17] C.A.C. Imbert, H.J. McQueen, Proc. of Int. Conf., CIM, 1996, p. 451.
[18] N.C. Mataya, V.E. Sackschewsky, Metall. Mater. Trans. A 25A (1994) 2737.
[19] H.J. McQueen, Mater. Sci. Eng. A A387–A389 (2004) 203.
[20] P.D. Hodgson, D.C. Collinson, B.A. Parker, in: J.J. Jonas, T.R. Bieler, K.J. Bowman (Eds.), Advances in Hot Deformation Textures and Microstructures, TMS, 1993, p. 41.